2908 *Chem. Mater.* **2010,** *22,* 2908–2915
DOI:10.1021/cm100236q

CHEMISTRY OF MATERIALS
Article

# Mechanosynthesis of the Orthorhombic Perovskites $ErMn_{1-x}Ni_xO_3$ ($x = 0, 0.1$). Processing and Characterization of Nanostructured Ceramics

A. Moure,*,† T. Hungría,‡ A. Castro,‡ J. Galy,§ O. Peña,⊥ J. Tartaj,† and C. Moure†

†*Instituto de Cerámica y Vidrio, CSIC, C/Kelsen, 5, 28049 Madrid, Spain,* ‡*Instituto de Ciencia de Materiales de Madrid, CSIC, c/Sor Juana Inés de la Cruz, 3 Cantoblanco, 28049 Madrid, Spain,* §*Centre d'Elaboration de Matériaux et d'Etudes Structurales, CNRS, 29 rue Jeanne Marvig, 31055 Toulouse, France, and* ⊥*Sciences Chimiques de Rennes, UMR 6226, Université de Rennes 1, Rennes, France*

*Received January 25, 2010. Revised Manuscript Received March 10, 2010*

Because of the Jahn−Teller effect and low tolerance factor, the only reported method to obtain $ErMnO_3$ materials with orthorhombic perovskite structure is to apply a high external pressure (on the order of GPa) at high temperature that transforms the stable room-temperature hexagonal structure to the more dense perovskite one. In this work, single-phase $ErMnO_3$ and $ErMn_{0.9}Ni_{0.1}O_3$ compositions with orthorhombic perovskite structure have been obtained for the first time by mechanosynthesis, after 24 h of milling in a tungsten carbide planetary mill. The high energy state achieved after the prolonged milling allows the perovskite structure to be isolated, instead of the habitual hexagonal one, without any external pressure. Subsequent thermal treatments transform the mechanosynthesized powder to the hexagonal structure at temperatures on the order of 1000 °C or higher. With the aim of obtaining ceramics with perovskite structure, spark plasma sintering (SPS) at 900 and 950 °C and 120 MPa was successfully tested. Ceramics processed by this way have densities greater than 90%.

## Introduction

Difference from the ternary oxides $REFeO_3$, RE = La, ... , Lu, and Y, which crystallize with a perovskite-type structure[1] in the whole, the manganese ternary oxides $LnMnO_3$ show two different stable polymorphs. For large rare-earth ionic radii from RE = La, ..., Ho, they crystallize also as orthorhombic perovskite-type, S.G. Pbnm (hereafter OP). When RE = Er, ..., Lu, and Y, with smaller ionic radii,[1] $LnMnO_3$ exhibits hexagonal symmetry (hereafter HS), with S.G. $P6_3cm$. This fact occurs despite the practically same ionic radius corresponding to $Fe^{3+}$ and $Mn^{3+}$[2] and therefore the same tolerance factor, $t$, for the perovskite-type structure, defined as

$$t = \frac{r_A + r_O}{\sqrt{2}(r_B + r_O)} \quad (1)$$

where $r_A$ and $r_B$ are the ionic radius of the A and B cation, respectively, and $r_O$ is that of the $O^{2-}$ anion.

The reason for the instability of the OP structure and therefore the formation of the hexagonal phase is the Jahn−Teller (JT) nature of the $Mn^{3+}$ cation. Because of the strong Hund's rule coupling, the manganese ions adopt a high spin configuration $t_{2g}^3e_g^1$. According to Jahn−Teller theorem, a distortion of the local octahedral environment, removing the degeneracy of the $e_g$ orbitals, is energetically favorable. This distortion is accomplished by lengthening two of the Mn−O bond trans to each other, which lowers the energy of the occupied $3d_z^2$ orbitals with respect to the empty $3d_{x^2-y^2}$ orbitals. The filled $3d_z^2$ orbitals form a zigzag pattern in the $xy$ plane, which leads to an expansion of the $a$ and $b$ unit-cell dimensions.[3,4] This is a cooperative effect explaining, along with the lowering of the tolerance factor, the appearance of HS for the small rare-earth cation compounds.[5] Superexchange interactions between $Mn^{3+}$ cations stabilize an A-type antiferromagnetic spin arrangement (ferromagnetic layers coupled antiferromagnetically to each other), with a semiconducting or isolating behavior.[6−8]

The suppression of this cooperative effect leads to the transition from HS → OP,[9−12] besides changes in the electrical and magnetic properties.[13,14] The suppression

*Corresponding author. E-mail: alberto.moure@icv.csic.es.

(1) Muller, O.; Roy, R. *The Major Ternary Structural Families*; Springer-Verlag: New York, 1974, p 357.
(2) Shannon, R. D. *Acta Crystallogr., Sect. A* **1976**, *32*, 751.
(3) Goodenough, J. B. *Phys. Rev.* **1955**, *100*(2), 564.
(4) Wollan, E. O. *Phys. Rev.* **1955**, *100*(2), 545.
(5) Pollert, E.; Krupicka, S.; Kiuzmikova., E. *J. Phys. Chem. Solids* **1982**, *43*(12), 1137.
(6) Peña, O.; Antunes, A. B.; Martínez, G.; Gil, V.; Moure, C. *J. Magn. Magn. Mater* **2007**, *310*, 159.
(7) Ye, F.; Lorenz, B.; Huang, Q.; Wang, Y. Q.; Sun, Y. Y.; Chu, C. W.; Fernandez-Baca, J. A.; Dai, P.; Mook, H. A. *Phys. Rev. B* **2007**, *76*, 060402.
(8) Huang, Y. H.; Fjellvg, H.; Karppinen, M.; Hauback, B. C.; Yamauchi, H.; Goodenough, J. B. *Chem. Mater.* **2006**, *18*(8), 2130.
(9) Moure, C.; Villegas, M.; Fernández, J. F; Tartaj, J.; Durán, P. *J. Mater. Sci.* **1999**, *34*, 2565.
(10) Iliev, M. N.; Lorenz, B; Litvinchuk, A. P.; Wang, Y. Q.; Sun, Y. Y.; Chu, C. W. *J. Phys.: Condens. Matter* **2005**, *17*(21), 3333.

 Published on Web 03/24/2010 

can be induced by formation of solid solutions (RE, Me)$MnO_3$, Me = Ca,Sr, Ba, and other divalent cations, which induces the appearance of $Mn^{4+}$ cations, with the subsequent lowering of the amount of $Mn^{3+}$ ones,[6,15−17] or RE(Mn,M)$O_3$, M = $Ni^{2+}$, $Co^{2+}$, $Cu^{2+}$, which induces the same effect that the above-described by two ways: appearance of $Mn^{4+}$ cations, and substitution of $Mn^{3+}$ by other non-JT cations.[6,18]

The OP manganites show a structure in which $c/\sqrt{2} < a < b$. This structure is associated to the strong orbit-lattice interaction of the $Mn^{3+}(d^4)$ ions. If the concentration of these cations is large, the cooperative distortion of the lattice due to the cooperative Jahn−Teller effect is predominant and the expected lattice deformation is then named as 0′-orthorhombic-type lattice. When the tolerance factor decreases, it is macroscopically reflected by the so-called O-type orthorhombic symmetry with $a < c/\sqrt{2} < b$. This steric effect leads to the cooperative buckling of the corner-shared octahedral.[19] Nevertheless, such steric effect seems to have a secondary role in the possible phase changes that occur in perovskite-type manganites. Progressive disappearance of $Mn^{3+}$ cations plays a relevant role in the phase changes, despite the increase in the tolerance factor caused, for example, by substituting a relatively small +3 rare-earth cation, Gd, Dy, Y, or Er, by a larger cation such as $Ca^{2+}$.[5,15−17]

The cell volume of the HS polymorph is higher than the one of the equivalent OP compounds such as $YFeO_3$. Therefore, it is possible to obtain the perovskite structure from hexagonal lattices by application of high pressures.[7,8,20,21] In fact, the more usual procedure is the preparation of the hexagonal phase by solid-state reaction between oxides or by a chemical route, as powder or as solid body, which is lately subjected to very high pressures, which can be as large as 5 GPa, at relatively high temperatures, 1100−1300 °C. To the author's best knowledge, the processing of orthorhombic pure phases corresponding to the smallest rare-earth cations, without applying any type of external pressure, has not been previously reported.

Mechanochemical method appears as an effective, economical and versatile way to produce a wide variety of functional materials. This process is based on chemical reactions that are mechanically activated by high-energy ball milling.[22,23] It has been successfully applied to obtain different oxides[24−26] or to stabilize high-temperature phases.[27] The process is able to produce oxide nanoparticles and also to obtain new oxides from a mixture of components, in a process called mechanosynthesis. It has been already applied to obtain some perovskite materials from two, three or even four oxides, such as $BaTiO_3$, (La,Ca)$MnO_3$, (La,Sr)(Ga,Mg)$O_3$, and many more. Some compounds that cannot be prepared by more conventional ways, such as solid-state reaction or chemical synthesis, have been obtained by this technique.[28,29]

In this work, the synthesis by high-energy ball milling of pure $ErMnO_3$ and the solid solution with $Ni^{2+}$ substituting $Mn^{3+}$ with a perovskite-type structure is shown. Nanostructured ceramics were processed by spark plasma sintering (SPS) at low temperatures (< 1000 °C) to stabilize the perovskite-type structure and to study their microstructure and magnetic features for this family of manganites, which have barely been studied (or not shown before, as for the $Ni^{2+}$ substitute material) due to the difficulties in their preparation.

## Experimental Section

Powders of $ErMn_{1-x}Ni_xO_3$, $x$ = 0, 0.1, were obtained by mechanosynthesis. The stoichiometric quantities of $Er_2O_3$, $Mn_2O_3$, NiO necessary to obtain 10 g of the powdered ceramic phases were placed in a tungsten carbide (WC) pot with seven also WC balls, 2 cm diameter (ball-to-powder weight ratio ~45/1). Mechanosynthesis was carried out with a Pulverisette 6 model Fritsch planetary mill operating at 300 rpm.

Evolution with different milling times of the precursors was monitored by Bragg−Brentano X-ray diffraction (XRD) with a Brüker AXS D8 Advance diffractometer. Cu $K_\alpha$ radiation ($\lambda$ = 1.5418 Å) and a $5 \times 10^{-2}$ ° $2\theta$ $s^{-1}$ scan rate were used. The obtained powder was characterized by scanning electron microscopy, SEM, in a FE-SEM (model Hitachi S-4700 working at 5 KV), and by transmission electron microscopy, TEM, which was carried out in a JEOL 2100 FEG working at 200 kV. Milled materials were uniaxially pressed and treated at temperatures between 900 and 1000 °C and later characterized by XRD. The phases were identified using a scanning rate of typically $3.3 \times 10^{-2}$ ° $2\theta$ $s^{-1}$. The lattice parameters were determined from the pattern of the thermal-treated at 900 °C samples, using a scanning rate of $2.1 \times 10^{-3}$ ° $2\theta$ $s^{-1}$. Si powder was employed as an internal standard. The lattice parameters were calculated

(11) Vega, D.; Polla, G.; Leyva, A. G.; Konig, P.; Lanza, H.; Esteban, A.; Aliaga, H.; Causa, M. T.; Tovar, M.; Alascio, B. *J. Solid State Chem.* **2001**, *156*(2), 458.
(12) Antunes, A. B.; Pena, O.; Moure, C.; Gil, V.; Andre, G. *J. Magn. Magn. Mater.* **2007**, *316*, 652.
(13) Gutiérrez, D.; Peña, O.; Durán, P.; Moure, C. *J. Eur. Ceram. Soc.* **2002**, *22*, 1257.
(14) Antunes, A. B.; Gil, V.; Moure, C.; Peña, O. *J. Eur. Ceram. Soc.* **2007**, *27*, 3927.
(15) Woodward, P. M.; Vogt, T.; Cox, D. E.; Arulraj, A.; Rao, C. N. R.; Karen, P.; Cheetham, A. K. *Chem. Mater.* **1998**, *10*, 3652.
(16) Sdiri, N.; Bejar, M.; Dhahri, E. *J. Magn. Magn. Mater.* **2007**, *311*, 512.
(17) Peña, O.; Bahout, M.; Gutierrez, D.; Duran, P.; Moure, C. *Solid State Sci.* **2003**, *5*, 1217.
(18) Moure, C.; Gutierrez, D.; Peña, O.; Duran, P. *J. Solid. State Chem.* **2002**, *163*, 377.
(19) Qian, T.; Tng, P.; Kim, B.; Lee, S. I; Shin, N.; Park, S.; Kim, B. G. *Phys. Rev. B* **2008**, *77*, 094423.
(20) Zhou, J. S.; Goodenough, J. B.; Gallardo-Amores, J. M.; Moran, E.; Alario-Franco, M. A.; Caudillo, R. *Phys. Rev. B* **2006**, *74*, 014422.
(21) Lorenz, B.; Wang, Y. Q.; Sun, Y. Y.; Chu, C. W. *Phys. Rev. B* **2004**, *70*, 212412.
(22) Bolarin, A. M.; Sánchez, F.; Palomares, S.; Aguilar, J. A.; Torres-Villaseñor, G. *J. Alloys Compd.* **2007**, *436*, 335.
(23) Muroi, M.; Street, R.; McCormick, P. G. *J. Solid State Chem.* **2000**, *152*, 503.
(24) Moure, A.; Castro, A.; Tartaj, J.; Moure, C. *J. Power Sources* **2009**, *188*, 489.
(25) Moure, A.; Castro, A.; Pardo, L. *Acta Mater.* **2004**, *52*, 945.
(26) Maca, K.; Cihlar, J.; Castkova, K.; Zmeskal, O.; Hadraba, H. *J. Eur. Ceram. Soc.* **2007**, *27*, 4345.
(27) Millán, P.; Rojo, J. M.; Castro, A. *Mater. Res. Bull.* **2000**, *35*, 832.
(28) Alguero, M.; Ricote, J.; Castro, A. *J. Am. Ceram. Soc.* **2004**, *87*, 772.
(29) Alguero, M.; Ricote, J.; Hungria, T.; Castro, A. *Chem. Mater.* **2007**, *19*, 4982.

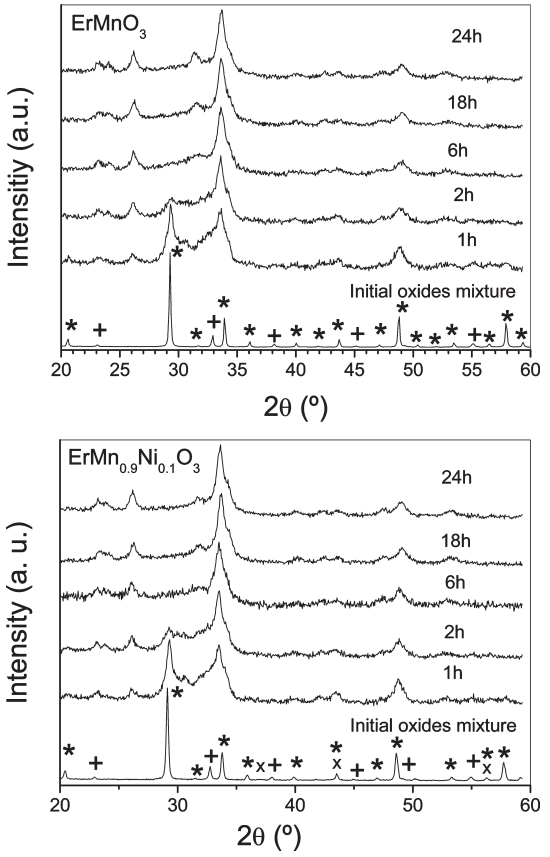


**Figure 1.** XRD patterns of the stoichiometric mixture of $Er_2O_3$, $Mn_2O_3$, NiO, precursor of $ErMnO_3$, and $ErMn_{0.9}Ni_{0.1}O_3$, after different milling times. (Initial oxides mixture: *, $Er_2O_3$; +, $Mn_2O_3$; ×, NiO).

using a mean square fit with all the peaks comprising between 20 and 70° 2$\theta$ angle range (16−18 peaks), which have been indexed according to the S.G. *Pbnm*. Correlation coefficients $>0.99$ and standard deviation sum $<1 \times 10^{-7}$ have been obtained for all the samples.

To study the structural change from OP to HS phase, approximately 1 g of the powders was uniaxially pressed in pellets with 0.8 mm diameter at 100 MPa and then isostatically pressed at 200 MPa. The shrinkage behavior was studied using a dilatometer Netzsch Gerätebau (model 402 EP, Selb-Bayern Germany) up to 1200 °C with a heating and cooling rate of 5 °C/min.

Ceramics with perovskite structure were processed by Spark Plasma Sintering (SPS). A cylindrical graphite die (8 mm inner diameter) was filled with the powder to be thus processed in a SPS 2080 Sumitomo apparatus. A pulsed direct current was passed through the die while an increasing uniaxial pressure was applied (up to 120 MPa) and the sample was heated to the final temperature (900 and 950 °C) at heating rates of 180−190 °C $min^{-1}$ approximately. The final sintering temperature and 120 MPa pressure were maintained for 1 min.

Density of the ceramics was measured by Archimede's method in distilled water at room temperature. After polishing and thermal etching, the microstructures of the sintered samples were examined by transmission electron microscopy on SPS-sintered thinned samples.

Magnetic measurements were performed on a Quantum Design MPMS-XL5 SQUID (superconducting quantum interference device) magnetometer between 2 and 300 K, under different applied fields (10 kOe for measurements in the paramagnetic state and 100 Oe for ZFC/FC cycles); magnetization M(H) was recorded up to $H = 50$ kOe at $T = 2$ K, with increasing and decreasing fields.

## Results and Discussion

Figure 1 shows the evolution of the initial oxide mixture after milling at different times to prepare $ErMnO_3$ and $ErMn_{0.9}Ni_{0.1}O_3$. Both present similar features. After 1 h of milling, the peaks corresponding to the OP phase begin to be visible, mixed with the ones of the starting oxides. After 6 h, it seems to be the majority phase. The situation is similar up to 24 h of milling. That is, the mechanosynthesis of the perovskite $Er_{1-x}Mn_xO_3$ can be achieved by milling in a relatively short time without any external pressure. The width and low intensity of the peaks point to the obtaining of a low particle size after milling. Figure 2 shows the TEM and SEM images of the mechanosynthesized powder after 24 h of milling corresponding to the Ni-doped powder, as representative of the observed in the samples. The nanometric character of the mechanosynthesized powder has been confirmed with a mean size of 23 nm, measured from TEM images from a population of more than 100 particles. The SEM images show a certain degree of agglomeration.

Thermal treatments in the range of 900−1000 °C were carried out on the mechanosynthesized powders to increase the crystallization degree of the OP phase and to study the range of its stability temperature. The XRD patterns for both nondoped and Ni-doped materials are shown in Figure 3. For the $ErMnO_3$ composition, a pure and well-crystallized OP phase is obtained at 900 °C. The HS phase begins to appear at increasing temperatures from 920 °C, and it is the unique detectable phase at 1000 °C. For the $ErMn_{0.9}Ni_{0.1}O_3$ composition, single OP phase is maintained even at 940 °C. Only at temperatures higher than 960 °C do reflections corresponding to the HS phase begin to appear. It is worth noting that, to the authors' best knowledge, the preparation of a single-phase material (either as OP or as HS) is achieved for the first time for the Ni- doped composition with low ($x = 0.1$) Ni concentration.

Figure 4 shows the lattice parameters calculated from XRD patterns, for the $ErMn_{1-x}Ni_xO_3$ ($x = 0, 0.1$) materials reported in this work, and at higher Ni content taken from.[30] The Ni incorporation induces the slight reduction of the a and b parameters (of about 0.15 and 1.5%, respectively) and the increase of c (about 0.60%), whereas the cell volume decreases. In any case, the perovskite polymorph exhibits a lower cell volume than the HS one and as a consequence a higher density. A monotonous decreasing of the distortion b/a at increasing Ni content is observed, indicating that the OP is less distorted. The XRD can be indexed as an orthorhombic perovskite within the spatial group Pbnm, type O′ with a change to O type for $x \geq 0.10$.

(30) Pena, O.; Antunes, A. B.; Baibich, M. N.; Lisboa-Filho, P. N.; Gil, V.; Moure, C. *J. Magn. Magn. Mater.* **2007**, *312*, 78.

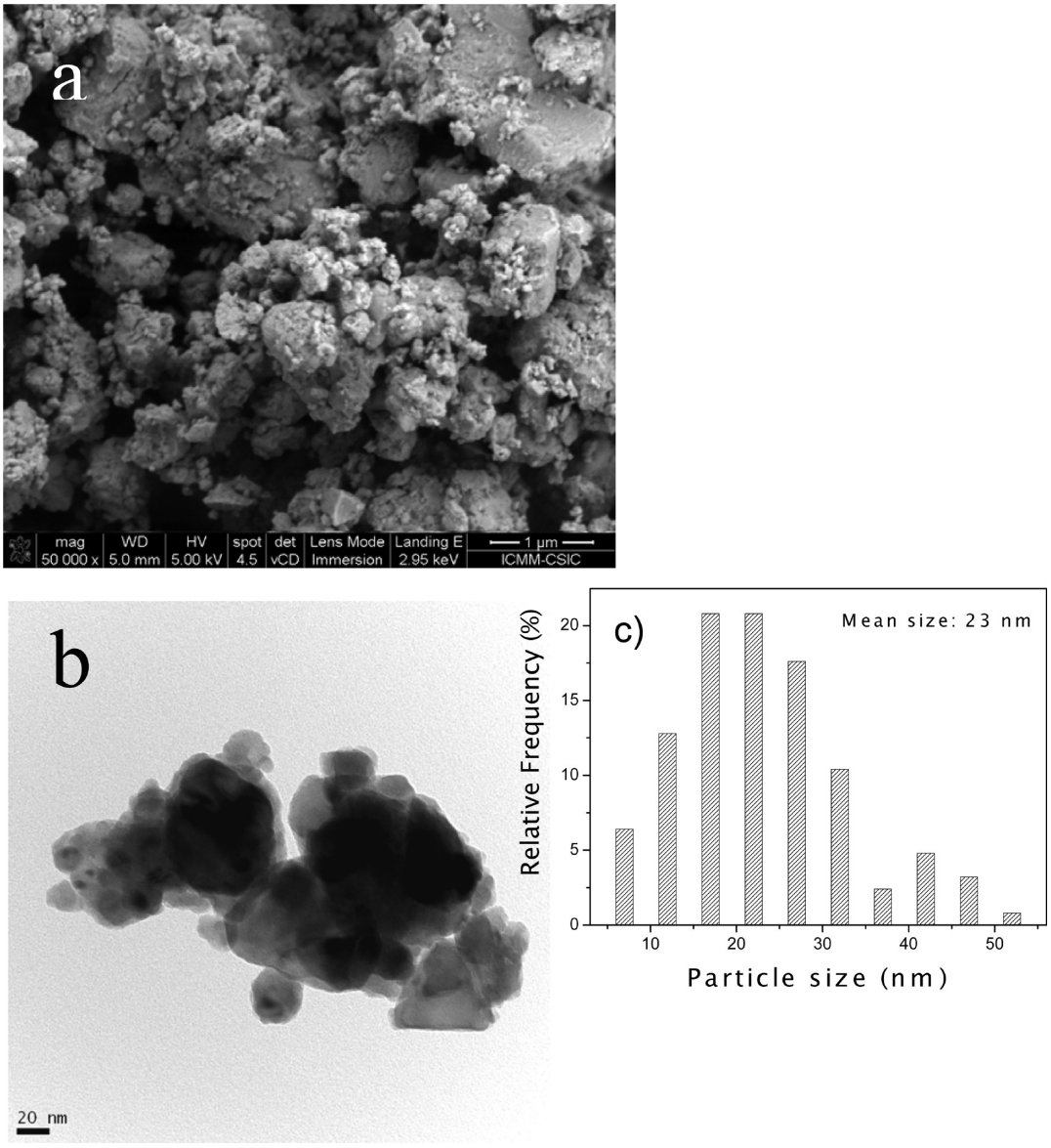


**Figure 2.** (a) SEM and (b) TEM micrographs of precursor powders of $ErMn_{0.9}Ni_{0.1}O_3$ ceramics after 24 h of milling, and (c) particle size distribution after measuring from TEM images.

As it was mentioned above, in the RE manganites, Jahn−Teller effect gives rise to a hard distortion of the OP structure that makes the HS phase to be energetically more favorable.[31] The ionic radii of the cations, reflected in the tolerance factor defined in eq 1, has a minor effect on the stabilization of such OP structure, which can be the reason for their more difficult obtention at decreasing ionic radii, within the late rare-earth manganites. The results shown here prove that the process by high energetic milling produces the mechanosynthesis of $ErMnO_3$ and $ErMn_{0.9}Ni_{0.1}O_3$ (obtained for the first time for this composition) with OP structure, being more stable for Ni-doped compositions. As these phases have been obtained up to now only by the application of high pressure that transforms the HS to the OP by changing the atomic Mn−O and R−O distances and modifying the Mn−O−Mn angles,[7,20,32] it can be supposed that similar effects are produced during the prolonged milling.

During the milling process, the impact of the balls on the mixture and the shear effect on the pot walls generate pressures that can be on the order of GPa,[33] similar to that necessary to occur HS → OP transformation. The main difference is that during milling, the pressure is not applied continuously but instead during the contacts, which have durations typically of $1 \times 10^{-5}$ s.[34] In this case, it is possible to define the process as a pressure-assisted-like synthesis, in which the initial reactives are oxides that react to form a perovskite at increasing milling times (Figure 1). During milling, the mechanical energy supplied helps the material with the highly distorted perovskite structure to be stabilized, similarly to the external pressure. Moreover, the milled powder has a

(31) Ren, C. Y. *Phys. Rev. B* **2009**, *79*, 125113.
(32) Tachibana, M.; Shimoyama, T.; Kawaji, H.; Atake, T.; Takayama-Muromachi, E. *Phys. Rev. B* **2007**, *75*, 144425.
(33) Suryanarayana, C. *Prog. Mater. Sci.* **2001**, *46*, 1.
(34) Suryanarayana; C. *Mechanical Alloying and Milling*, Ed.; Marcel Dekker: New York, 2004; p 188.

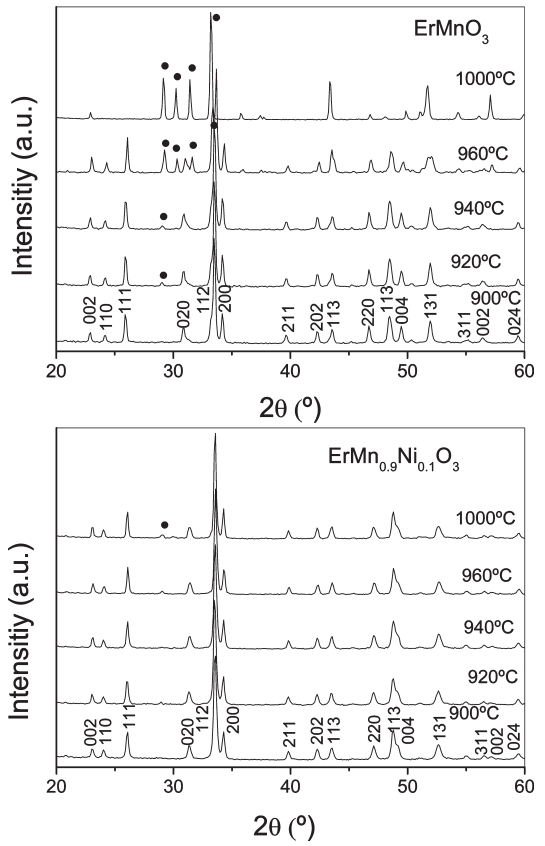


**Figure 3.** XRD patterns after several thermal treatments of $ErMnO_3$ and $ErMn_{0.9}Ni_{0.1}O_3$ mechanosynthesized after 24 h of milling (•, peaks corresponding to the HS phase).

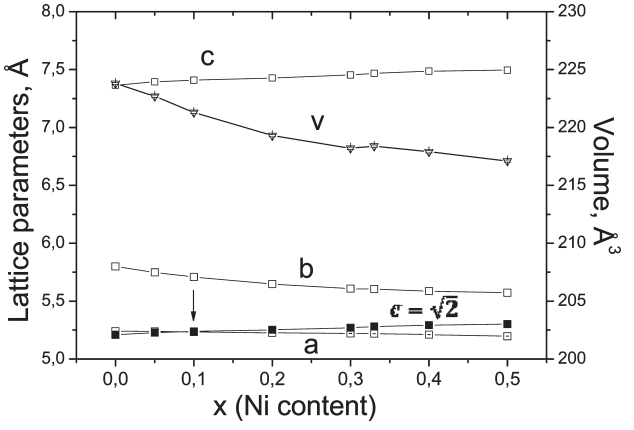


**Figure 4.** Lattice parameters and unit-cell volume calculated from XRD patterns, for the $ErMn_{1-x}Ni_xO_3$ ($x$ = 0, 0.1) materials reported in this work, and at higher Ni content taken from.[30] The arrow indicates the change from O′ to O structure.

high average crystalline strain because of the disorder and defects introduced by the impacts. It has been reported that this strain has a hydrostatic like component that facilitates the synthesis of OP structure materials with a high degree of distortion.[29] In these conditions, the OP structure is attained and stabilized, despite the Jahn−Teller effect imposing a very high instability of the structure. In conclusion, mechanosynthesis allows more dense polymorphs to be stabilized at room temperature, even when they are in a metastable state, as in the case of the materials shown in this work. Subsequent thermal treatments relax the strained state after mechanosynthesis, and the more stable HS structure is formed.

**Table I. Comparison of Lattice and Strain Parameters of $ErMnNiO_3$ Materials with OP Structure Obtained by Several Methods (Errors in Lattice Parameters Calculation: ±0.0001 Å)**

| | synthesis method | *a* (Å) | *b* (Å) | *c* (Å) | *c*/*a* | *b*/*a* |
|---|---|---|---|---|---|---|
| this work | mechanosynthesis | 5.2410 | 5.7980 | 7.3650 | 1.41 | 1.11 |
| Ye et al. ref 7. | 3.5 GPa, 1100 °C | 5.2273 | 5.7922 | 7.3308 | 1.40 | 1.11 |
| Zhou et al. ref 20. | 4 GPa, 1000 °C | 5.2419 | 5.8257 | 7.3397 | 1.40 | 1.11 |
| Tachibana et al. ref 30. | 6 GPa, 1300 °C | 5.2395 | 5.8223 | 7.3357 | 1.40 | 1.11 |
| Alonso et al. ref 34. | chemistry | 5.2262 | 5.7932 | 7.3486 | 1.41 | 1.11 |
| Ren et al. ref 29. | theoretic | 5.2440 | 5.8650 | 7.3430 | 1.40 | 1.12 |

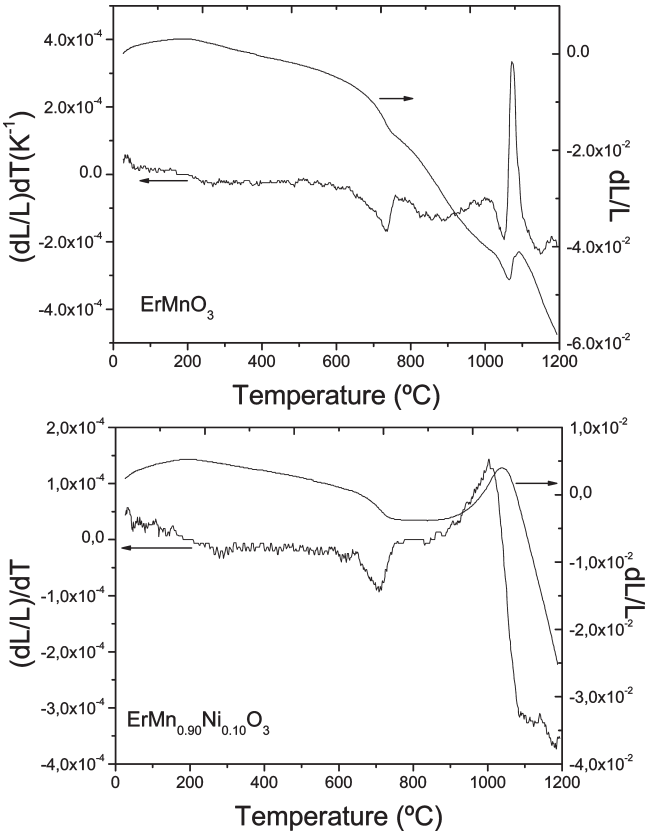


**Figure 5.** Shrinkage and shrinkage rate of green pellets of $ErMnO_3$ and $ErMn_{0.9}Ni_{0.1}O_3$ compositions mechanosynthesized after 24 h of milling.

The comparison of the lattice parameters obtained in this work with the ones reported in the literature for $ErMnO_3$ composition[7,20,32,35] is shown in Table I. The theoretical parameters for the OP structure calculated in[31] are also added as a reference. The ones corresponding to this work were calculated in the mechanosynthesized powder and thermal treated at 900 °C. The results show a good agreement with those previously reported for this composition.

Figure 3 shows that the Ni-doped perovskite has a higher temperature existence range than the nondoped phase. The substitution of $Ni^{2+}$ diminishes the amount of

(35) Alonso, J. A.; Martinez-Lope, M. J.; Casais, M. T.; Fernandez-Diaz, M. T. *Inorg. Chem.* **2000**, *39*, 917.

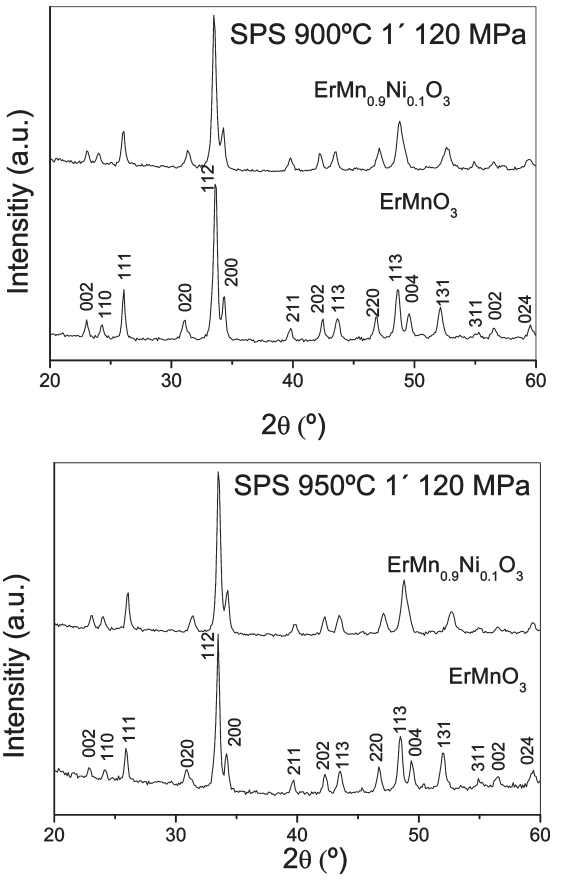


**Figure 6.** XRD patterns of SPS ceramics of $ErMnO_3$ and $ErMn_{0.9}Ni_{0.1}O_3$ processed at 900 and 950 °C.

$Mn^{3+}$ in B sites, reducing the perovskite instability because of the Jahn−Teller effect,[36] as is observed by the structural change from O′ to O (Figure 4). Anyway, the high pressure applied during milling allows the distorted perovskite to be stabilized as it occurs for the nondoped material. The reduction of the distortion due to the presence of $Ni^{2+}$ cations increases the difference of energy between the perovskite structure and the stable hexagonal phase, thus increasing its stability temperature range.

Figure 5 shows the shrinkage and shrinkage rate for $ErMnO_3$ and $ErMn_{0.9}Ni_{0.1}O_3$ compositions. The measurements were carried out without any external pressure. The transition from OP to HS is distinguished as the expansions in the Figure 5, located at temperatures higher than 1000 °C. The transition is more rapid in the nondoped perovskite, as the peak in the maximum shrinkage rate is narrower than for the Ni-doped ceramic. This is in good agreement with that shown in Figure 3, where the OP phase completely transforms to HS within a range of 100 °C, taking into account that the dilatometric is a dynamic measurement in contrast with the thermal treatments, which results are shown in Figure 3. It is observed from Figure 5 that the transition occurs during the ceramic densification. This obviously limits the temperatures at which the ceramics can be sintered, making thus difficult to have dense ceramics with perovskite structure by conventional sintering. With the aim of overcoming this problem, SPS was employed to process ceramics with these characteristics.

Figure 6 shows the XRD patterns of the nondoped and Ni-doped ceramics processed by SPS at 900 and 950 °C. These are the highest successfully checked temperatures. The coupling of high heating rate, external pressure application and the OP → HS phase transition led to a violent explosion of the die when sintering at temperatures higher than 950 °C is tried. All the peaks in Figure 6 can be indexed as corresponding to the OP structure. In contrast to the shown in Figure 3, the perovskite structure remains at 950 °C. This is due to the pressure applied during the SPS processes, which allows the metastable OP to be maintained at higher temperatures than if no pressure is applied (see Figure 3). In any case, the value of this pressure is in the order of the MPa, in contrast to the GPa order and high temperatures applied in refs 7,20, and 32 necessary to transform HS structure to the OP one. The difference is that no transformation occurs in this case, as the ceramics are processed from a powdered precursor that already has the orthorhombic-perovskite structure.

The high degree of densification achieved by SPS of mechanosynthesized precursors was measured by Archimedes' method. Relative densities higher than 90% are achieved, with a highest value of 93% for the $ErMn_{0.9}Ni_{0.1}O_3$ ceramics. This is a consequence of the nanometric character and high sinterability of the mechanosynthesized powdered phases, which made it possible to attain these high density values with a high microstructural homogeneity. The high concentration of defects introduced by the prolonged milling enhances the mass transport and increases the densification of the ceramics even at these low densification temperatures.[37]

The reduced sintering temperature has a direct consequence on the microstructure of the ceramics. Figure 7 shows the TEM images corresponding to $ErMnO_3$ ceramics processed by SPS at 900 (Figure 7a) and 950 °C (Figure 7b). It is observed that the ceramics are nanostructured in both cases, with all the grain sizes largely lower than 100 nm. The increase in temperature from 900 to 950 °C does not have much influence on the grain growth, as it is observed in the grain size distributions (shown in the insets of the Figure), centered on 35 and 45 nm for the ceramics processed at 900 and 950 °C, respectively. In fact, the mean values measured in both cases from the distributions are approximately the same. The limited grain growth is related to the high heating rates achieved by Spark Plasma Sintering, being in the order of 180−190 °C $min^{-1}$ in this work. The grain coarsening mechanisms by surface diffusion, predominant at low temperature regime, are not favored. Sintering takes place at conditions where grain boundary and volume diffusion are predominant, resulting in high densifications and limited grain growth.[38] To the authors' best

(36) Moure, C.; Gutierrez, D.; Pena, O.; Duran, P. *J. Solid State Chem.* **2002**, *163*, 377.
(37) Algueró, M.; Amorín, H.; Hungría, T.; Galy, J.; Castro, A. *Appl. Phys. Lett.* **2009**, *94*, 012902.
(38) Hungria, T.; Galy, J.; Castro, A. *Adv. Eng. Mater.* **2009**, *11*, 615.

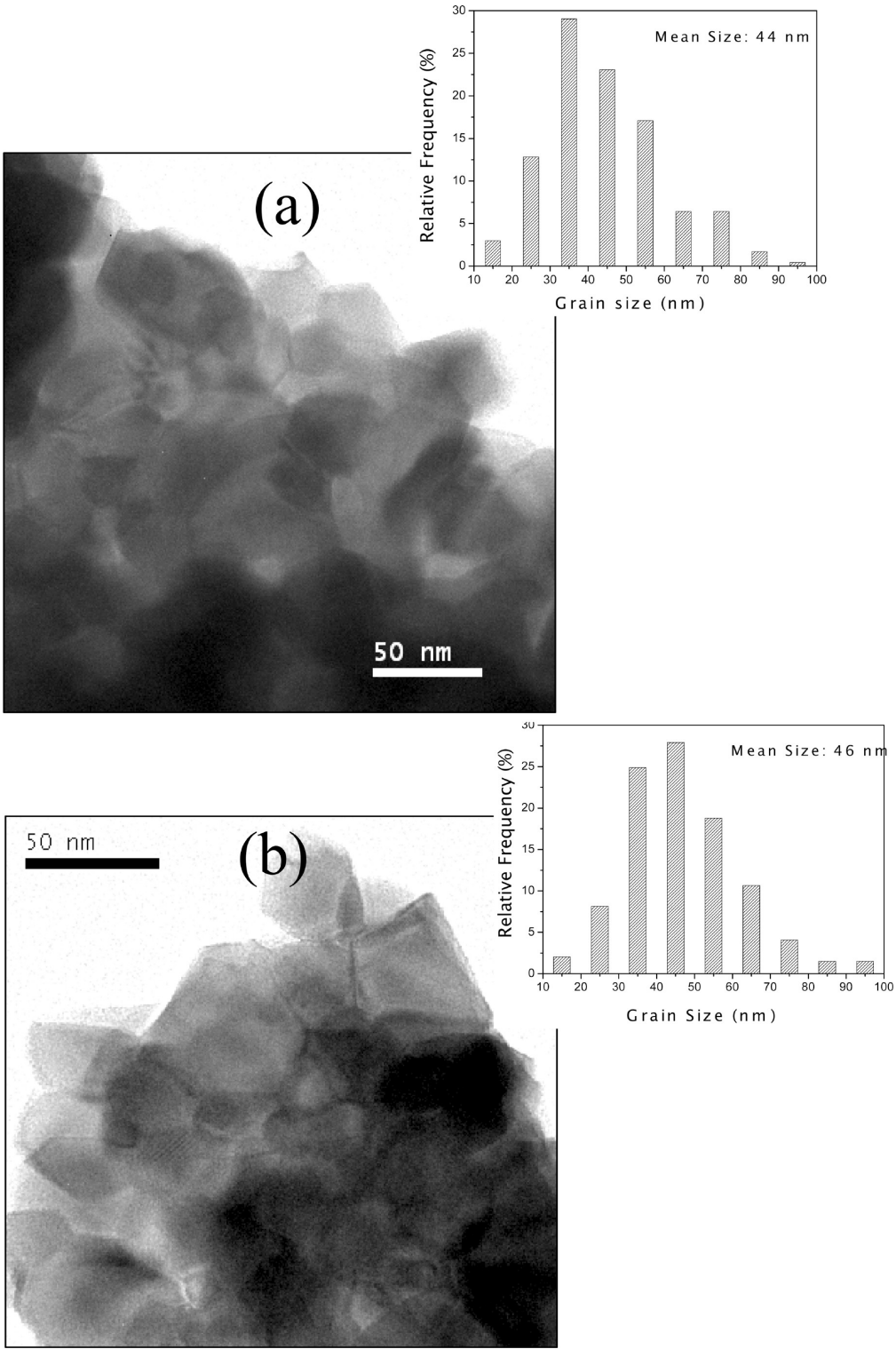


**Figure 7.** TEM images of grains corresponding to $ErMnO_3$ ceramics processed by SPS at (a) 900 and (b) 950 °C, and the corresponding grain size distributions.

knowledge, this is the first report of $ErMn_{1-x}Ni_xO_3$ nanostructured ceramics.

Figure 8 shows the magnetic behavior of the $ErMn_{1-x}Ni_xO_3$ ($x = 0, 0.1$) materials processed by SPS. Comparing with ref 30 it can be observed that the magnetic behavior correlates well with that observed for higher Ni-doped region ($x = 0.20$) of the OP solid solution $ErMn_{1-x}Ni_xO_3$, obtained by conventional solid-state synthesis. The paramagnetic region, predominantly due to the $Er^{3+}$ cation, is described by a Curie−Weiss behavior (insets, Figure 8, upper panels) with effective moments $\mu_{eff} = 10.5$ and $10.6\ \mu_B$ ($\pm 0.1$) for $x = 0$ and 0.1, respectively, compared to $\mu_{eff} = 10.27\ \mu_B$ ($\pm 0.15$) for $x = 0.2$,[30] whereas the Curie−Weiss temperature shows a continuous variation from antiferromagnetic interactions ($\Theta = -19$ and $-14$ K ($\pm 0.5$), for $x = 0$ and 0.1,

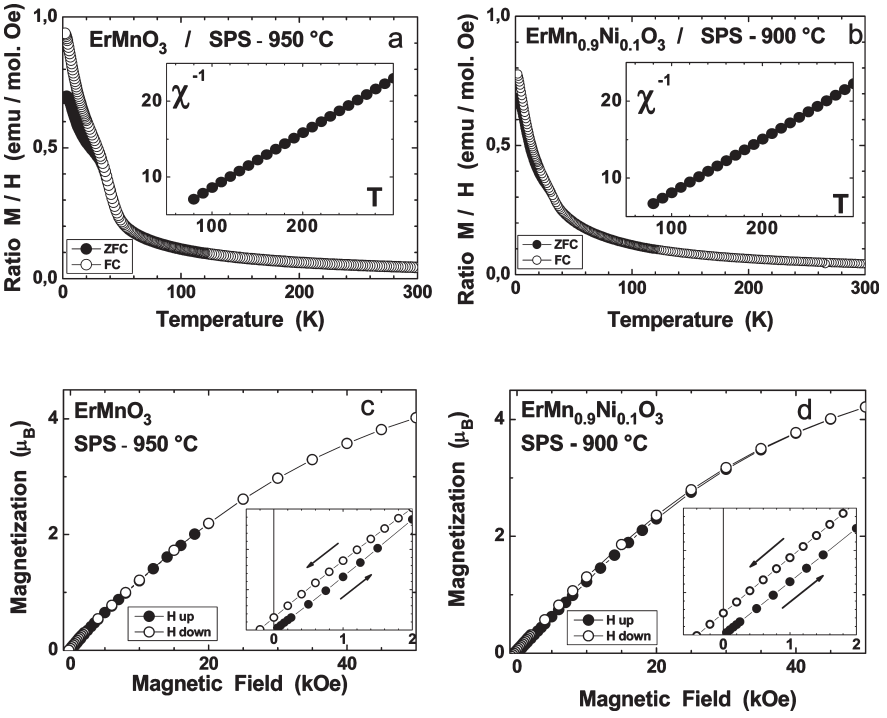


**Figure 8.** Field cooling and zero-field cooling (FC and ZFC curves, respectively) of ceramics processed by SPS: (a) $ErMnO_3$ 950 °C and (b) $ErMn_{0.9}Ni_{0.1}O_3$ 900 °C (insets: inverse of the susceptibility of the corresponding ceramics); and magnetization loops of ceramics processed by SPS at 2 K: (c) $ErMnO_3$ 950 °C and (d) $ErMn_{0.9}Ni_{0.1}O_3$ 900 °C.

respectively) toward a ferromagnetic behavior ($\Theta = -6$ and $+1.8$ K ($\pm$ 0.5), for $x = 0.2$ and 0.3, respectively[30]).

The temperature dependence of the magnetization is described by the zero-field-cooled (ZFC)/field-cooled (FC) cycles shown in the main upper panels, shown in Figure 8. A reversible behavior is observed in the paramagnetic regime $T > T_{rev}$, where $T_{rev} = 33$ and 30 K, for $x = 0$ and 0.1, respectively, compared to the value of 18 K reported for $x = 0.2$.[30] This characteristic temperature $T_{rev}$ is ascribed to the presence of small amounts of $Mn^{4+}$ and not to ferromagnetic $Ni^{2+}-Mn^{4+}$ interactions[39] (which are absent for $x = 0$, and quite diluted in samples with $x = 0.1$ and 0.2), in contrast to the strong ferromagnetic interactions observed for $x = 0.33$ ($T_c = 40$ K) and $x = 0.40$ ($T_c = 62$ K) (see Figure 6 in ref 30). This is confirmed by the magnetization M(H) measurements performed at $T = 2$ K (lower panels, Figure 8) for the SPS ceramics of this work: only a slight increase of the coercive field is observed when Ni is incorporated to the perovskite structure, while the predominant exchange interaction comes from the $Mn^{3+}/Mn^{4+}$ pairs, quite diluted for $0 \leq x \leq 0.2$. According to the results reported in ref 30 ferromagnetic order becomes important at $x(Ni) \geq 0.33$.

## Conclusions

The high energy introduced by impacts in a high energetic ball milling allows single-phase orthorhombic perovskites, with $ErMn_{1-x}Ni_xO_3$ composition ($x = 0$, 0.1), to be obtained for the first time by a straightforward solid-state method. This avoids the application of the external pressure, in the order of GPa, that is often used to transform the hexagonal stable structure to the orthorhombic perovskite one. Small Ni-doping levels, at the Mn position, help the perovskite-like structure to be retained, probably due to the reduction in the Jahn–Teller effect.

The metastable character of $ErMn_{1-x}Ni_xO_3$ ($x = 0$, 0.1) OP phase, which transforms to the stable HS polymorph at relatively low temperature, compel the use of spark plasma sintering to obtain ceramics with high density (>90%) at low temperatures (≤950 °C). This method allows the grain size to be maintained at the nanoscale range, in a nonpreviously reported result, always keeping the OP, with Pbnm symmetry.

Magnetic behavior correlates to that previously reported in this solid solution, with $ErMn_{1-x}Ni_xO_3$ compositions ($x \geq 0.20$), obtained by conventional solid-state synthesis, proving the effectiveness of the mechanosynthesis as a simpler route to develop such materials with orthorhombic structures instead of the usual ones using high pressures on the order of GPa.

**Acknowledgment.** This work was supported by Spain PROFIT CIT-120000-2007-50 and MICINN MAT2008-06785-C02-02-E. A.C. and T.H. acknowledge the financial support of the Spanish MICINN (Project MAT2007-61884). A.M. and T.H. are indebted to the CSIC (MICINN) of Spain for the "Junta de Ampliación de Estudios" contracts (refs JAEDOC087 and JAEDOC082, respectively). The authors are grateful for the technical support provided by Ms. I. Martínez (ICMM). The authors also thank the assistance of the PFN2, Toulouse, France, where the SPS experiments were performed.

(39) Blasse, G. *J. Phys. Chem. Solids* **1965**, *26*, 1969.